ADP-ribosylhydrolase activity of Chikungunya virus macrodomain is critical for virus replication and virulence

Robert Lyle McPherson[a,1], Rachy Abraham[b,1], Easwaran Sreekumar[b,1,2], Shao-En Ong[c], Shang-Jung Cheng[a], Victoria K. Baxter[b,d], Hans A. V. Kistemaker[e], Dmitri V. Filippov[e], Diane E. Griffin[b,3], and Anthony K. L. Leung[a,f,3]

[a]Department of Biochemistry and Molecular Biology, Bloomberg School of Public Health, Johns Hopkins University, Baltimore, MD 21205; [b]W. Harry Feinstone Department of Molecular Microbiology and Immunology, Bloomberg School of Public Health, Johns Hopkins University, Baltimore, MD 21205; [c]Department of Pharmacology, University of Washington, Seattle, WA 98195; [d]Department of Molecular and Comparative Pathobiology, School of Medicine, Johns Hopkins University, Baltimore, MD 21205; [e]Department of Bio-organic Synthesis, Leiden University, Einsteinweg 55, 2333 CC Leiden, The Netherlands; and [f]Department of Oncology, School of Medicine, Johns Hopkins University, Baltimore, MD 21205

Contributed by Diane E. Griffin, January 5, 2017 (sent for review October 20, 2016; reviewed by William Lee Kraus and Susan R. Weiss)

Chikungunya virus (CHIKV), an Old World alphavirus, is transmitted to humans by infected mosquitoes and causes acute rash and arthritis, occasionally complicated by neurologic disease and chronic arthritis. One determinant of alphavirus virulence is nonstructural protein 3 (nsP3) that contains a highly conserved MacroD-type macrodomain at the N terminus, but the roles of nsP3 and the macrodomain in virulence have not been defined. Macrodomain is a conserved protein fold found in several plus-strand RNA viruses that binds to the small molecule ADP-ribose. Prototype MacroD-type macrodomains also hydrolyze derivative linkages on the distal ribose ring. Here, we demonstrated that the CHIKV nsP3 macrodomain is able to hydrolyze ADP-ribose groups from mono(ADP-ribosyl)ated proteins. Using mass spectrometry, we unambiguously defined its substrate specificity as mono(ADP-ribosyl)ated aspartate and glutamate but not lysine residues. Mutant viruses lacking hydrolase activity were unable to replicate in mammalian BHK-21 cells or mosquito *Aedes albopictus* cells and rapidly reverted catalytically inactivating mutations. Mutants with reduced enzymatic activity had slower replication in mammalian neuronal cells and reduced virulence in 2-day-old mice. Therefore, nsP3 mono(ADP-ribosyl)hydrolase activity is critical for CHIKV replication in both vertebrate hosts and insect vectors, and for virulence in mice.

macrodomain | ADP-ribosylation | mass spectrometry | virulence | viral replication

Alphaviruses are members of the *Togaviridae* family of icosahedral, enveloped, message-sense RNA viruses that are maintained in a natural cycle between vertebrate and invertebrate hosts. Alphavirus infection can result in human disease with viruses originating from the "Old World" primarily causing rash and arthritis and "New World" causing encephalitis. However, recent strains of Chikungunya virus (CHIKV), an "Old World" alphavirus, cause neurologic disease as well as rash and arthritis (1). CHIKV originates from sub-Saharan Africa but has spread to Southeast Asia, Europe, and more recently the Americas, where its transmission by *Aedes aegypti* and *Aedes albopictus* vectors has the potential to cause infection in tens of millions of people (1). There are no approved therapeutics for CHIKV partly because of a poor understanding of the basic molecular underpinnings of its infection and replication cycle.

The 5′ ORF of the alphaviral genome encodes four nonstructural proteins (nsPs) that function in replication of the viral RNA and production of the subgenomic RNA (2, 3). nsPs are translated as two polyproteins (nsP123 and nsP1234) that form replication complexes tethered to cytoplasmic vacuoles formed from modified endosomal membranes. The polyproteins are processed into individual proteins by a papain-like protease in the C-terminal portion of nsP2. nsP1 has methyl and guanylytransferase activities, is palmitoylated, and binds the replication complex to membranes. The N-terminal domain of nsP2 has helicase, ATPase, GTPase, methyltransferase, and 5′ triphosphatase activity. nsP4 is the RNA-dependent RNA polymerase (4).

The function of nsP3 has been more enigmatic. nsP3 is found in replication complexes and cytoplasmic nonmembranous granules. It induces the membrane remodeling necessary for the formation of cytoplasmic vacuoles and regulates RNA synthesis in a cell type-dependent manner (5). In vivo, nsP3 is a determinant of neurovirulence in mice (6–10). nsP3 has three major domains, a highly conserved N-terminal macrodomain, a central zinc-binding region, and a poorly conserved, unstructured, acidic, and highly phosphorylated C-terminal domain. The C-terminal domain interacts with and regulates the function of many cellular proteins to impact signaling, viral replication, and stress granule assembly (11–15). The roles of the N-terminal macrodomain and central zinc-binding region are less well characterized.

Macrodomains are a conserved protein fold observed from archaea to higher eukaryotes characterized by their binding to the small molecule ADP-ribose and its derivatives (16–18). Macrodomains are part of the nsPs in a subset of positive-strand

Significance

Viral outbreaks can be sudden and result in devastating social and economic consequences. Chikungunya virus (CHIKV) outbreaks of rash, arthritis, and neurologic disease have occurred in Africa, Asia, Europe, and the Americas. There are no licensed vaccines to prevent or drugs to treat CHIKV infection, and the mechanisms of disease generation are poorly understood. Here, we identify a macrodomain-containing CHIKV protein with enzymatic ADP-ribosylhydrolase activity that is critical for virulence in mammals and define the substrate specificity of this enzyme. Given the conservation of viral macrodomains in all alphaviruses and coronaviruses, our study may guide the design of small molecule chemical compounds that block hydrolase activity for treatment of a range of virus infections.

Author contributions: R.L.M., R.A., E.S., D.E.G., and A.K.L.L. designed research; R.L.M., R.A., E.S., S.-E.O., S.-J.C., and V.K.B. performed research; H.A.V.K. and D.V.F. contributed new reagents/analytic tools; R.L.M., R.A., E.S., S.-E.O., D.E.G., and A.K.L.L. analyzed data; and R.L.M., D.E.G., and A.K.L.L. wrote the paper.

Reviewers: W.L.K., The University of Texas Southwestern Medical Center at Dallas; and S.R.W., University of Pennsylvania.

The authors declare no conflict of interest.

[1]R.L.M., R.A., and E.S. contributed equally to this work.

[2]Present address: Viral Disease Biology Program, Rajiv Gandhi Centre for Biotechnology, Thiruvananthapuram, Kerala 695014, India.

[3]To whom correspondence may be addressed. Email: anthony.leung@jhu.edu or dgriffi6@jhmi.edu.

This article contains supporting information online at www.pnas.org/lookup/suppl/doi:10.1073/pnas.1621485114/-/DCSupplemental.

RNA viruses, including alphaviruses, coronaviruses, and hepatitis E virus (16–18). Study of viral macrodomain function has provided conflicting results with respect to their importance for virus replication. In general, viruses with mutations in the ADP-ribose–binding site of the macrodomain replicate well in most tissue culture cells, but often exhibit attenuated replication in differentiated cells and decreased virulence in vivo (10, 19–23). For instance, mutations of conserved residues in the ADP-ribose–binding region of the Sindbis virus macrodomain impair replication and RNA synthesis in neurons and attenuate neurovirulence in mice (10). Similarly, mutation of the macrodomain of coronavirus nsP3 at a conserved site attenuates virulence and replication in mice and affects induction of and sensitivity to IFN and inflammatory cytokines (19, 20, 22, 23).

Viral macrodomains are of the MacroD subfamily, which includes archaeal *Af*1521 and human MacroD2. Recently, our group and others have found that some MacroD-type macrodomains bind and hydrolyze ADP-ribose monomers conjugated to the side chains of protein residues, a posttranslational modification known as ADP-ribosylation (23–27). ADP-ribose groups can be attached singly as mono(ADP-ribose) (MAR) or in branched or linear polymeric chains as poly(ADP-ribose) (PAR) by the enzymatically active members of a family of 17 ADP-ribosyltransferases, commonly known as poly(ADP-ribose) polymerases (PARPs) (28–30). ADP-ribosylation involves the transfer of ADP-ribose from NAD^+ onto a range of amino acids, including aspartate (D), glutamate (E), and lysine (K) (30–32). Until recently, it has not been possible to identify the site of ADP-ribosylation by mass spectrometry (MS) (reviewed in refs. 31 and 33). Sequence alignment of the CHIKV macrodomain with the known human MAR hydrolase MacroD2 revealed that the residues required for catalysis are conserved (refs. 25 and 26 and *SI Appendix*, Fig. S1). In this study, we determined that the CHIKV macrodomain possesses MAR hydrolase activity and unambiguously identified its substrate specificity by MS. Furthermore, using recombinant viruses with targeted mutations in the macrodomain, we demonstrate that hydrolase function is important for viral replication in neuronal cells in vitro and for neurovirulence in mice.

Results

CHIKV nsP3 Macrodomain Removes Mono(ADP-Ribose) from Modified Aspartate and Glutamate, but Not Lysine Residues. To determine whether the macrodomain of CHIKV nsP3 ($nsP3^{MD}$) possesses MAR hydrolase activity, we subcloned $nsP3^{MD}$ from the CHIKV vaccine strain 181/Clone 25 (181/25) into a bacterial expression plasmid and purified recombinant $nsP3^{MD}$ to homogeneity for in vitro characterization. We incubated the catalytic domain of PARP-10 ($PARP10^{CD}$) with ^{32}P-NAD^+ to generate ^{32}P-MARylated $PARP10^{CD}$ as a substrate for a MAR hydrolase assay. ^{32}P-MARylated $PARP10^{CD}$ was incubated with buffer alone, $nsP3^{MD}$, or the positive control MacroD2, for 1 h at 37 °C followed by analysis by SDS/PAGE and autoradiography (Fig. 1*A*). There was a significant decrease in the intensity of ^{32}P-MARylated $PARP10^{CD}$ in samples containing MacroD2 and $nsP3^{MD}$, whereas buffer alone resulted in minimal loss of ^{32}P signal. We further characterized $nsP3^{MD}$ by monitoring the time dependence of this decrease in ^{32}P signal (Fig. 1*B*). $nsP3^{MD}$ kinetics were slower than MacroD2 under the tested reaction conditions; yet, both enzymes decreased the signal from ^{32}P-MARylated $PARP10^{CD}$ by upwards of 40% within 10 min. Of note, ~10% of the ^{32}P signal remained even after the demodification was allowed to proceed for 2 h, suggesting that certain ADP-ribosylated sites were more resistant to the hydrolase activity of MacroD2 and nsP3 than others. The reaction products at the 1-h time point were further analyzed by thin-layer chromatography (TLC) and autoradiography, showing the ^{32}P-labeled product released from modified $PARP10^{CD}$ had the same retention factor as pure ADP-ribose (*SI Appendix*, Fig. S2). Therefore, CHIKV

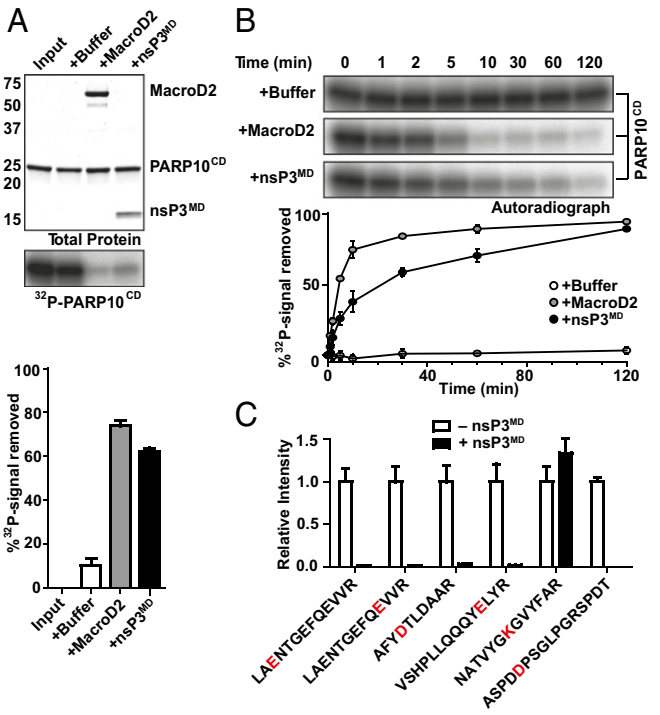

Fig. 1. CHIKV $nsP3^{MD}$ removes ADP-ribose from MARylated $PARP10^{CD}$. (*A* and *B*) Total protein stain, autoradiography, and quantification of ^{32}P-MARylated $PARP10^{CD}$ demodification reactions by MacroD2 or CHIKV $nsP3^{MD}$ at 1 h time-point (*A*) and over a time course of 2 h (*B*). (*C*) Quantification of LC-MS extracted ion chromatograms for phosphoribosylated $PARP10^{CD}$ peptides, where modified residues are denoted in red.

$nsP3^{MD}$ possesses enzymatic activity for hydrolysis of ADP-ribose groups from MARylated substrates.

Biochemical and mutagenesis data have inferred that human and archaeal MAR hydrolases remove ADP-ribose groups from acidic residues (24–26), but the specificity of viral MAR hydrolases has not been examined. To identify the amino acid residues demodified by $nsP3^{MD}$, we first determined the sites of modification on MARylated $PARP10^{CD}$ by using a phosphodiesterase-based MS approach that can identify different amino acid ADP-ribosylation sites (24, 34–36). In brief, MARylated $PARP10^{CD}$ was incubated with a phosphodiesterase that cleaves the pyrophosphate of ADP-ribose to leave a phosphoribose tag at the original site of modification. Proteins were then digested and phosphoribosylated peptides were enriched by immobilized metal affinity chromatography and sequenced by liquid chromatography (LC)–MS/MS to identify sites of modification. This approach identified six highly confident phosphoribosylated sites on $PARP10^{CD}$, based on our criteria of >99% site localization probability and high fragment coverage of the modification site in MS/MS spectra, at D, E, or K residues (*SI Appendix*, Fig. S3 and Table S1). To test whether $nsP3^{MD}$ was capable of removing MAR from these modified residues, we incubated $PARP10^{CD}$ with either $nsP3^{MD}$ or buffer alone, followed by treatment with phosphodiesterase and proteases, and subjected these samples to LC–MS/MS analyses. To quantify the differences in intensity of modified peptides under these different conditions, we extracted ion chromatograms from three technical replicates for individual phosphoribosylated $PARP10^{CD}$ peptides (*SI Appendix*, Fig. S4) and quantified the resulting peaks (Fig. 1*C*). There was a significant reduction in the ion intensity of peptides with phosphoribosylated D and E residues in samples incubated with $nsP3^{MD}$. However, no reduction of the PARP10 peptide modified at K916 residue was observed (Fig. 1*C*). Together, these data show that

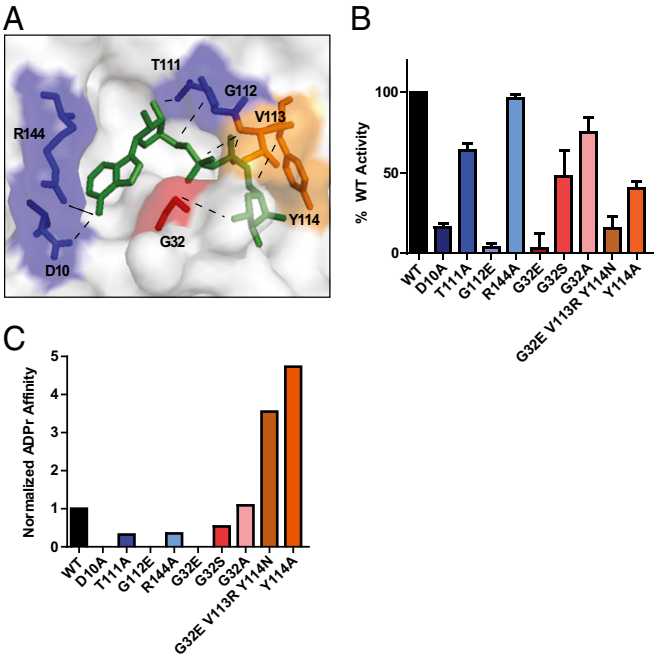

Fig. 2. Characterization of CHIKV nsP3^{MD} mutants that are defective in ADP-ribose–binding and/or MAR hydrolase activity. (*A*) Active site of CHIKV nsP3^{MD} bound to ADP-ribose (37) highlighting residues targeted in this study. (*B*) Quantitative representation of MAR hydrolase activity of nsP3^{MD} mutants relative to nsP3^{MD} WT. Assays were performed in triplicate, buffer control was subtracted, and obtained values were normalized to activity levels of nsP3^{MD} WT. Representative raw data shown in *SI Appendix*, Fig. S5. (*C*) Quantitative representation of ADP-ribose affinity of nsP3^{MD} mutants normalized to nsP3^{MD} WT. Raw data shown in Table 1 and *SI Appendix*, Fig. S7.

nsP3^{MD} is capable of removing MAR from modified aspartate and glutamate, but not lysine residues on PARP10^{CD}.

Generating nsP3^{MD} Mutants Defective in MAR Hydrolysis and ADP-Ribose Binding. To determine whether the MAR hydrolase activity of nsP3^{MD} plays a role in the replication and/or virulence of CHIKV, we generated and biochemically characterized nsP3^{MD} mutants before incorporating the mutations into recombinant viruses for further studies in cells and mice. We interrogated the solved crystal structure of ADP-ribose–bound CHIKV nsP3^{MD} to identify active site residues that make critical contacts with the free small molecule that, if mutated, would be predicted to disrupt the enzyme's ability to bind to and hydrolyze MARylated substrates (Fig. 2*A* and ref. 37). We mutated residues D10, G32, T111, G112, and R144 because of their broad distribution in the active site and diverse contacts with free ADP-ribose (37). These mutations differentially affected the MAR hydrolase activity of recombinant nsP3^{MD} with R144A having little effect, T111A reducing enzymatic activity to ~64% of WT levels, and D10A, G112E, and G32E diminishing enzymatic activity to background levels (Fig. 2*B*, Table 1, and *SI Appendix*, Fig. S5). Previous studies of human MacroD2 have shown that mutations other than glutamate substitutions at the position equivalent to G32 can fine-tune the MAR hydrolase activity in vitro (26). Following this logic, we additionally generated and characterized nsP3^{MD} G32A and G32S in vitro and found that these mutant enzymes possessed ~75% and ~48% of WT levels, respectively (Fig. 2*B*, Table 1, and *SI Appendix*, Fig. S5). Mutation to G32D or G32Q, like G32E, reduces hydrolase activity of the nsP3^{MD} to negligible levels (*SI Appendix*, Fig. S6).

As for most studied macrodomains (37–40), nsP3^{MD} binds to free ADP-ribose in vitro as measured by isothermal titration calorimetry (Fig. 2*C*, Table 1, and *SI Appendix*, Fig. S7), which is an informative proxy for its affinity for MARylated peptides (41). Mutations at positions equivalent to nsP3 D10, G32, and G112 in MacroD2 disrupt ADP-ribose binding (26), and these nsP3^{MD} mutants were also defective in ADP-ribose binding (Fig. 2*C*, Table 1, and *SI Appendix*, Fig. S7). Like G32E, nsP3^{MD} G32D and G32Q were also defective in ADP-ribose binding (*SI Appendix*, Fig. S6). Because they also possessed similarly low levels of hydrolase activity, both electrostatic repulsion and steric hindrance likely contribute to the disruption of ADP-ribose binding and MAR hydrolase activity of nsP3^{MD}. Given the similarity among D, E, and Q mutants at G32, G32E was chosen as a representative mutation for further characterization. For R144A, T111A, G32S, and G32A, we were able to measure the affinities of nsP3^{MD} for ADP-ribose and found that these mutants also had reduced binding to ADP-ribose (Fig. 2*C*, Table 1, and *SI Appendix*, Fig. S7). Therefore, any potential phenotypic differences observed in viruses carrying these mutations could be attributed to deficient MAR hydrolase activity and/or ADP-ribose binding (defined as category 1 mutants).

Table 1. Compiled quantitation data from in vitro, cell culture, and in vivo experiments on nsP3 WT and mutants of CHIKV 181/25 strain

CHIKV strain	ADP-ribose K_D, μM	Hydrolase activity, %	Virus progeny	Sequencing	Replication (NSC-34), %	Mortality in mice, %	Mean days of death
WT	22.9 ± 3.7	100	Yes		100	100	2.5
Category 1							
D10A	NDB	16.1 ± 2.3	No	Reverted to WT	N/A	N/A	N/A
G32A	21.0 ± 3.7	75.3 ± 9.3	Yes		7	58	6.9
G32S	42.9 ± 17.7	48.0 ± 16.0	Yes		4	4	Undefined
G32E	NDB	3.8 ± 9.1	No	Reverted to WT	N/A	N/A	N/A
T111A	71.4 ± 11.5	64.1 ± 4.0	Yes		<1	44	5.3
G112E	NDB	3.7 ± 2.5	No	Reverted to WT	N/A	N/A	N/A
R144A	64.9 ± 14.9	96.2 ± 2.3	No	Reverted to WT	N/A	N/A	N/A
Category 2							
Y114A	4.84 ± 0.69	40.6 ± 4.2	Yes		16 (Delayed)	75	5.3
G32E V113R Y114N	6.46 ± 1.25	15.0 ± 7.2	No	Reverted to either G32A V113R Y114N or V113R Y114N	N/A	N/A	N/A

Hydrolase activity is calculated as a percentage of nsP3 WT activity after subtraction of buffer control. Replication rate is defined as the number of plaques in a mutant divided by the number of plaques in WT. CHIKV 181/25$^{E2\ I12T\ R82G}$ and mutant derivatives were used in mouse experiments. N/A, not available; NDB, no detectable binding.

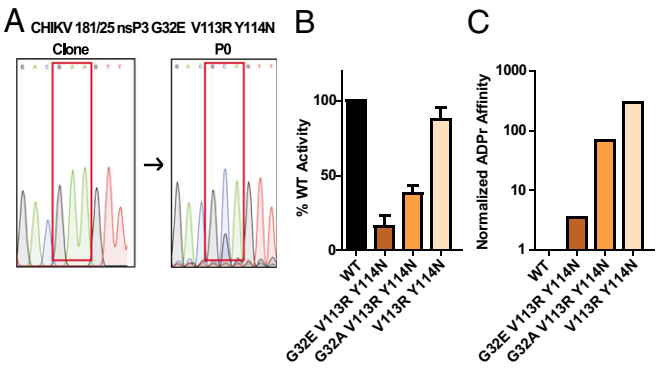

Fig. 3. Characterization of CHIKV 181/25 nsP3 G32E V113R Y114N mutant revertants. (*A*) Sequencing chromatogram of nsP3 G32E V113R Y114N-containing plasmid clones and virus particles produced at P0 from BHK-21 cells. (*B*) Quantitative representation of MAR hydrolase activity of nsP3^{MD} mutants relative to nsP3^{MD} WT. Assays were performed in triplicate, buffer control was subtracted, and obtained values were normalized to activity levels of nsP3^{MD} WT. Representative raw data shown in *SI Appendix*, Fig. S9. (*C*) Quantitative representation of ADP-ribose affinity of nsP3^{MD} mutants normalized to nsP3^{MD} WT. Raw data shown in Table 1 and *SI Appendix*, Fig. S9.

To unambiguously determine the importance of the MAR hydrolase activity of nsP3^{MD} in CHIKV replication and virulence, we sought to generate nsP3^{MD} mutants with impaired hydrolase activity that still bound to free ADP-ribose (category 2 mutants). Studies of other macrodomains have shown that mutations in V113 and Y114 disrupt various hydrolase activities without affecting ADP-ribose binding (26, 42). Therefore, we generated nsP3^{MD} G32E V113R Y114N and nsP3^{MD} Y114A and showed that they have higher affinity for ADP-ribose than the WT protein while possessing ∼15% and ∼41% of WT enzymatic activity, respectively (Figs. 2 *B* and *C*, Table 1, and *SI Appendix*, Figs. S5 and S7).

nsP3^{MD} MAR Hydrolase Activity and ADP-Ribose Binding Are Critical for CHIKV Replication in Cell Culture. Characterized mutations were introduced into a plasmid containing the full-length cDNA of the RNA genome of CHIKV 181/25 (43). The plasmid was in vitro transcribed, and the resulting RNA was transfected into BHK-21 cells for virus production. Sequencing of the RNA of the resulting viral particles revealed that viruses produced from transfection of CHIKV 181/25 RNA with D10A, G32E, and G112E had reverted the mutated residue back to the original residue (Table 1 and *SI Appendix*, Fig. S8). Furthermore, G32E reversion occurred with both codons for glutamate (GAA and GAG) and in two different cell lines, mammalian BHK-21 and mosquito *Aedes albopictus* C6/36, both lacking an IFN response (*SI Appendix*, Fig. S8) (44). Intriguingly, CHIKV 181/25 did not tolerate the R144A mutation despite the presence of near WT levels of MAR hydrolase activity and the ability to bind ADP-ribose in vitro (Fig. 2 *B* and *C*, Table 1, and *SI Appendix*, Fig. S5), suggesting that macrodomain properties other than ADP-ribose binding and hydrolase activity may be important for CHIKV replication. Notably, R144 is not conserved in all alphaviruses, suggesting a function potentially specific to CHIKV (*SI Appendix*, Fig. S1). Interestingly, viruses produced from the G32E V113R Y114N cDNA mutated to a mixture of ∼80% G32A V113R Y114N and ∼20% V113R Y114N (Fig. 3*A*). Biochemical characterization of these nsP3^{MD} mutants showed that their enzymatic activity was partially restored, and their affinity for ADP-ribose was increased ∼70- to 300-fold compared with WT (Fig. 3 *B* and *C* and *SI Appendix*, Fig. S9). These data suggest that CHIKV replication is incompatible with nsP3^{MD} mutations that severely attenuate MAR hydrolase activity, even when ADP-ribose binding is restored with the additional mutations V113R Y114N. Together, these results indicate that ADP-ribosylhydrolase activity in nsP3^{MD} is critical for CHIKV replication.

To determine the importance of nsP3 MAR hydrolase activity for CHIKV replication, we infected mouse neuronal NSC-34 cells with the viable recombinant nsP3^{MD} mutant viruses at a multiplicity of infection (MOI) of 10 and measured virus production by plaque assay in Vero cells. All of the assayed mutants replicated less well than the parent virus (Fig. 4*A* and Table 1). Viruses with single mutations at G32 to either A or S replicated with similar kinetics, but with lower virus yields that correlated with the loss of MAR hydrolase activity and ADP-ribose binding in vitro, implicating one or both of these biochemical characteristics of nsP3 as important for viral replication. Virus yield was further lowered with the T111A mutant, which has an intermediate hydrolase activity between G32A and G32S mutant but a much lower affinity to ADP-ribose (Fig. 4*A* and Table 1). These data indicate that limiting ADP-ribose binding, which is likely required for hydrolase activity, further reduces the replication of these enzymatically impaired mutants. Replication of the Y114A mutant, which has a stronger affinity for ADP-ribose than WT but 40% of hydrolase activity, was distinct in that it displayed delayed replication kinetics and a lower yield compared with the parent virus (Fig. 4*A* and Table 1). These data show that for virus replication even enhanced levels of nsP3 ADP-ribose binding do not compensate for impaired MAR hydrolase activity.

Mutations Affecting nsP3^{MD} MAR Hydrolase Activity and ADP-Ribose Binding Attenuate CHIKV Virulence in Mice. Next, we assessed the importance of the MAR hydrolase activity and ADP-ribose binding of nsP3 in vivo. First, we reversed attenuating mutations I12T and R82G in the E2 glycoprotein of CHIKV 181/25 to generate a recombinant CHIKV strain virulent for newborn mice (CHIKV 181/25$^{E2\ I12T\ R82G}$) (45). nsP3 mutations were then introduced into this more virulent background and 1,000 pfu of the resulting viruses were used for intracranial infection of 2-d-old mice (Fig. 4*B*). Mice infected with CHIKV 181/25$^{E2\ I12T\ R82G}$ all died 2–4 d after infection (mean day-of-death; MDOD = 2.5). All viruses with mutated nsP3 macrodomains had reduced virulence. Mutants G32A and G32S had mortalities of 58% (MDOD = 6.9, $P < 0.0001$) and 4% ($P < 0.0001$), respectively (Fig. 4*B* and Table 1). Notably, T111A had intermediate virulence between

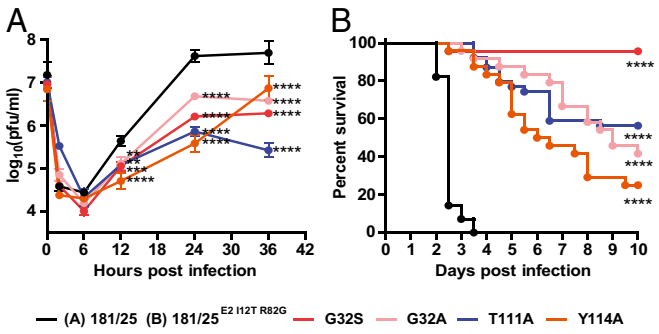

Fig. 4. Macrodomain mutations in CHIKV nsP3 impair replication kinetics in cell culture and attenuate virulence in vivo. (*A*) Replication of CHIKV 181/25 WT and nsP3 mutants in NSC-34 cells infected at an MOI of 10. Average data of three independent experiments are presented. Error bars indicate SEMs. $^{**}P < 0.01$; $^{***}P < 0.001$; $^{****}P < 0.0001$; 181/25 vs. nsP3 mutants. Dunnett's multiple comparisons test. (*B*) Mortality of 2-d-old neonatal mice (n = 24–28 per virus strain) after intracranial infection with CHIKV 181/25$^{E2\ I12T\ R82G}$ or nsP3 mutants. Percentage of survival was plotted by using Kaplan–Meyer analysis and compared with log rank test. Data were pooled from two independent experiments, $^{****}P < 0.0001$; WT vs. nsP3 mutants.

G32A and G32S with 44% mortality (MDOD = 5.3, $P < 0.0001$; Fig. 4*B* and Table 1). Compared with the parent, the Y114A mutant had less hydrolase activity but ~fivefold more ADP-ribose–binding ability and was the most virulent of the mutants (75%, MDOD = 5.3, $P < 0.0001$; Fig. 4*B* and Table 1). These results indicate that MAR hydrolase activity is critical for CHIKV virulence in vivo. However, comparison between two mutants, Y114A and G32S, that have comparable hydrolase activity but differ in ADP-ribose–binding ability (Fig. 2 *B* and *C* and Table 1) indicated that the virulence of mutant CHIKV can be increased with stronger than WT ADP-ribose–binding ability of nsP3.

Discussion

Using the macrodomain from the CHIKV nsP3 protein, we demonstrated (*i*) the substrate specificity of a viral macrodomain and (*ii*) that the macrodomain MAR hydrolase activity is critical for virus replication and virulence. Using MS, we unambiguously determined that CHIKV nsP3^{MD} is able to remove ADP-ribose groups from modified aspartate and glutamate, but not lysine residues (Fig. 1). Previously, mutagenesis and biochemical data deduced that MacroD2 can hydrolyze MARylated acidic residues such as glutamate and aspartate (25, 26), and our proteomics data inferred that archaeal macrodomain *Af*1521 specifically removes ADP-ribose groups from modified glutamates (24). Here, we definitively showed that a macrodomain is able to distinguish and remove different classes of ADP-ribosylation from a single protein. Given that nsP3^{MD} is critical for virulence of CHIKV, such substrate specificity of its MAR hydrolase activity indicates that a certain class of ADP-ribosylation is critical for host–virus interactions.

Next, we took a structure-function approach to determine the importance of the MAR hydrolase activity of nsP3^{MD}. Mutations in the nsP3 ADP-ribose–binding site reduced its MAR hydrolase activity while simultaneously reducing its affinity for free ADP-ribose (category 1 mutants). To delineate the importance of these two properties of nsP3 in cells and in vivo, we generated mutants with additional mutations at V113 and Y114 that retained ADP-ribose binding but lacked enzymatic activity (category 2 mutants) (Fig. 2 and Table 1). Intriguingly, we were unable to produce viable CHIKV of either category with the catalytically inactivating D10A, G32E, G112E, and G32E V113R Y114N mutations. For G32E-based mutants, there was rapid selection for mutation of this residue back to either glycine or alanine accompanied by partial restoration of the nsP3 MAR hydrolase activity (Fig. 3), indicating that this enzymatic activity is critical for CHIKV replication. Notably, both cell lines used for virus recovery lacked a functional IFN pathway, suggesting that MAR hydrolase activity of nsP3 may play a fundamental role in CHIKV replication independent of an innate IFN response. Because reversion occurred in both mammalian and mosquito cells, MAR hydrolase activity is critical for viral replication in both vertebrate host and invertebrate vector. Alphavirus replication begins with the delivery of genomic RNA into the cytoplasm, followed by the translation and processing of nsPs to produce functional replication complexes (2, 3). The replication complexes generate the minus strand RNA that serves as a template for transcription of full-length genomic and subgenomic RNAs. The structural proteins required for packaging of the virus are translated from the subgenomic RNA. Given that nsP3 is part of the replication complex and no viable mutant virus particles were made from the catalytically dead mutants even at passage 0, CHIKV must be under strong selective pressure to maintain functional MAR hydrolase activity during these initial steps in viral replication.

We were able to generate viable CHIKV mutants with partially reduced nsP3 MAR hydrolase activity and determined that category 1 mutant viruses lacking both binding and hydrolase activity were attenuated for replication in cell culture and virulence in neonatal mice. Additionally, category 2 mutant viruses lacking only hydrolase activity had impaired replication in NSC-34 cells, leading us to conclude that MAR hydrolase, but not ADP-ribose binding, by the nsP3^{MD} is critical for viral replication in cell culture. Unexpectedly, category 2 mutants were more virulent in neonatal mice than category 1 mutants with similar levels of MAR hydrolase activity. Y114A and G32S have comparable levels of MAR hydrolase activity, but the former has a 10-fold higher affinity for ADP-ribose in vitro. In vivo, mice infected with CHIKV Y114A had 75% mortality, whereas mice infected with CHIKV G32S had only 4% mortality (Fig. 4). These data suggest that strong ADP-ribose binding of nsP3 can partially rescue the reduced virulence of CHIKV that results from diminished MAR hydrolase activity. The reasons for decreased virulence in mice require further investigation but likely relate to the ability of the viruses to replicate in cells of the nervous system. The reason that relative replication efficiency in NSC-34 cells does not completely predict relative virulence in mice may be due to differences in the types of cells infected, in the innate or adaptive responses to infection, or to differences linked to virulence-determining amino acid changes in E2.

The role of MARylation in the host response to viral infection is not understood. Recent work has demonstrated that the MAR transferase PARP-12 is up-regulated by alphaviral infection to inhibit host and viral protein synthesis dependent on its enzymatic activity (46, 47). Of note, PARP-9, PARP-14, and PARP-15, of which the latter two are MAR transferases, bear typical antiviral gene signatures and possess ADP-ribose–binding macrodomains that undergo recurrent positive selection and are described as being "locked in antagonistic 'arms races' with viral factors" (48). MARylation could play an antiviral role in the host cell and present an environment in which the MAR hydrolase activity of a viral protein could inhibit this antiviral response. Therefore, controlling the critical level of ADP-ribosylation may be at the forefront of the battle between the virus and the host antiviral response.

Materials and Methods

PARP10^{CD} Demodification Assay. For each reaction, 1 μg of PARP10^{CD} was automodified with 0.5 μCi ^{32}P NAD$^+$ for 30 min at 30 °C in automodification buffer (20 mM Tris·HCl pH 7.5, 50 mM NaCl, 5 mM $MgCl_2$,10 mM β-mercaptoethanol). Excess ^{32}P NAD$^+$ was removed by desalting by gravity flow in a Micro Bio-spin Column (Bio-Rad) into demodification buffer (25 mM Tris·HCl pH 7.0, 200 mM NaCl, 10 mM β-mercaptoethanol). MARylated PARP10^{CD} was incubated with equimolar amounts of macrodomain proteins for 1 h at 37 °C unless otherwise indicated. Reactions were stopped with SDS/PAGE Running Buffer, and samples were subjected to SDS/PAGE on a 14% (wt/vol) Tris-Glycine gel (Invitrogen). Total protein levels were analyzed with SimplyBlue Safe Stain (Invitrogen), and ^{32}P signal was visualized by autoradiography. TLC analysis of reaction products was performed as described (27).

Isothermal Titration Calorimetry. The binding of ADP-ribose to nsP3^{MD} was studied by isothermal titration calorimetry (ITC) using a VP-ITC instrument (MicroCal). Proteins were dialyzed into ITC buffer (20 mM Hepes pH 7.0, 100 mM NaCl) overnight at 4 °C. Dialyzed protein and ADP-ribose were respectively diluted to 40 μM and 1 mM in the dialyzed ITC buffer. Protein solution (1.4 mL) was loaded into the sample cell and titrated with 24 10-μL injections after an initial 2-μL injection of ligand. The heat evolved at 25 °C after each injection was obtained by integration of the calorimetric signal. The data were analyzed on Origin 5.0 software and fitted by using a one binding-site model.

PARP10^{CD} Site Identification. Purified PARP10^{CD} was automodified with 1 mM NAD$^+$ for 2 h at 37 °C in automodification buffer (20 mM Tris·HCl pH 7.5, 50 mM NaCl, 5 mM $MgCl_2$, 10 mM β-mercaptoethanol). Excess NAD$^+$ was removed by gel filtration using a Superose 12 10/300 GL column (Pharmacia). For each sample, 35 μg of PARP10^{CD} was incubated with or without 35 μg of nsP3^{MD} for 1 h at 37 °C followed by treatment with 35 μg of hsNudT16a for 2 h at 37 °C (34). Samples were then denatured, reduced, and alkylated in denaturing buffer (100 mM Tris·HCl pH 7.0 at 37 °C, 1.5 M guanidine-HCl, 1 mM $CaCl_2$, 5 mM TCEP, 10 mM CAM) at 37 °C for 10 min. Denatured proteins were digested with 2 μg of LysC for 3 h at 37 °C, followed by 2 μg of trypsin overnight at 37 °C. Peptides were desalted, phosphoenriched, and analyzed by LC–MS/MS, and MaxQuant searches were performed as described (36).

Cell Culture and Viral Replication Studies. The murine neuronal NSC-34 cell line, a kind gift from Neil Cashman, University of British Columbia, Vancouver, BC, Canada (49) was grown in DMEM supplemented with heat-inactivated 10% (vol/vol) FBS, L-glutamine (2 mM), penicillin (100 U/mL), and streptomycin (100 μg/mL) (Invitrogen), at 37 °C in a 5% CO_2 incubator. Baby hamster kidney 21 (BHK-21) and Vero cells were grown in DMEM/10% (vol/vol) FBS as above. *A. albopictus* clone (C6/36) cells were grown in DMEM/10% (vol/vol) FBS as above at 28 °C in a 5% CO_2 incubator. Virus stocks were grown in BHK-21 cells, and titers were determined by plaque assay in Vero cells. NSC-34 cells were infected at a MOI of 10 in DMEM/1% FBS for 1 h, and supernatant fluids were titered by plaque formation on Vero cells. Data are plotted as the means of the $\log_{10}$ values of pfu ± SEM.

Animals and Infection. Timed pregnant CD-1 mice were purchased from Charles River Laboratories and maintained in an animal BSL3 facility. At postnatal day 2, mouse pups were infected intracranially with 1,000 pfu of virus in 10 μL of PBS while under isoflurane anesthesia. Pups were monitored twice daily for 10 d. Survival was analyzed by using Kaplan–Meyer survival curves and log rank test. All experiments were performed according to a protocol approved by the Johns Hopkins University Institutional Animal Care and Use Committee and followed guidelines of the National Institutes of Health and the US Public Health Service Policy on Humane Care and Use of Laboratory Animals.

ACKNOWLEDGMENTS. We thank Naomi Forrester for the cDNA for CHIKV vaccine strain 181/25; Bernhard Lüscher for sharing pGEX-4T1 GST-PARP10cd; and Joel Moss, Scott Bailey, Jennifer Kavran, and members of the D.E.G. and A.K.L.L. laboratories for their helpful suggestions. This work was supported by a Johns Hopkins Catalyst Award (to A.K.L.L.); a Journal of Cell Science Travelling Fellowship (to R.L.M.); a Fulbright-Nehru Academic and Professional Excellence Fellowship from the US-India Educational Foundation (to E.S.); the Netherlands Organization for Scientific Research (to D.V.F.); and research grants from the Johns Hopkins University School of Medicine Sherrilyn and Ken Fisher Center for Environmental Infectious Disease (to D.E.G.) and R01GM104135 (to A.K.L.L.), R01GM104135S1 (to R.L.M.), and R01AR065459 (to S.-E.O.) from the National Institutes of Health.

1. Weaver SC, Lecuit M (2015) Chikungunya virus and the global spread of a mosquito-borne disease. *N Engl J Med* 372(13):1231–1239.
2. Strauss JH, Strauss EG (1994) The alphaviruses: Gene expression, replication, and evolution. *Microbiol Rev* 58(3):491–562.
3. Schwartz O, Albert ML (2010) Biology and pathogenesis of chikungunya virus. *Nat Rev Microbiol* 8(7):491–500.
4. Coffey LL, Beeharry Y, Bordería AV, Blanc H, Vignuzzi M (2011) Arbovirus high fidelity variant loses fitness in mosquitoes and mice. *Proc Natl Acad Sci USA* 108(38): 16038–16043.
5. LaStarza MW, Lemm JA, Rice CM (1994) Genetic analysis of the nsP3 region of Sindbis virus: Evidence for roles in minus-strand and subgenomic RNA synthesis. *J Virol* 68(9): 5781–5791.
6. Saul S, et al. (2015) Differences in processing determinants of nonstructural polyprotein and in the sequence of nonstructural protein 3 affect neurovirulence of Semliki Forest virus. *J Virol* 89(21):11030–11045.
7. Fros JJ, et al. (2015) Mosquito Rasputin interacts with chikungunya virus nsP3 and determines the infection rate in Aedes albopictus. *Parasit Vectors* 8:464.
8. Tuittila M, Hinkkanen AE (2003) Amino acid mutations in the replicase protein nsP3 of Semliki Forest virus cumulatively affect neurovirulence. *J Gen Virol* 84(Pt 6): 1525–1533.
9. Tuittila MT, Santagati MG, Röyttä M, Määttä JA, Hinkkanen AE (2000) Replicase complex genes of Semliki Forest virus confer lethal neurovirulence. *J Virol* 74(10): 4579–4589.
10. Park E, Griffin DE (2009) The nsP3 macro domain is important for Sindbis virus replication in neurons and neurovirulence in mice. *Virology* 388(2):305–314.
11. Fros JJ, et al. (2012) Chikungunya virus nsP3 blocks stress granule assembly by recruitment of G3BP into cytoplasmic foci. *J Virol* 86(19):10873–10879.
12. Thaa B, et al. (2015) Differential PI3K-Akt-mTOR activation by Semliki Forest and chikungunya virus, dependent on nsP3 and connected to replication complex internalisation. *J Virol*, 10.1128/JVI.01579-15.
13. Fros JJ, et al. (2010) Chikungunya virus nonstructural protein 2 inhibits type I/II interferon-stimulated JAK-STAT signaling. *J Virol* 84(20):10877–10887.
14. Neuvonen M, et al. (2011) SH3 domain-mediated recruitment of host cell amphiphysins by alphavirus nsP3 promotes viral RNA replication. *PLoS Pathog* 7(11): e1002383.
15. Park E, Griffin DE (2009) Interaction of Sindbis virus non-structural protein 3 with poly (ADP-ribose) polymerase 1 in neuronal cells. *J Gen Virol* 90(Pt 9):2073–2080.
16. Gorbalenya AE, Koonin EV, Lai MM (1991) Putative papain-related thiol proteases of positive-strand RNA viruses. Identification of rubi- and aphthovirus proteases and delineation of a novel conserved domain associated with proteases of rubi-, alpha- and coronaviruses. *FEBS Lett* 288(1-2):201–205.
17. Koonin EV, et al. (1992) Computer-assisted assignment of functional domains in the nonstructural polyprotein of hepatitis E virus: delineation of an additional group of positive-strand RNA plant and animal viruses. *Proc Natl Acad Sci USA* 89(17): 8259–8263.
18. Rack JGM, Perina D, Ahel I (2016) Macrodomains: Structure, function, evolution, and catalytic activities. *Annu Rev Biochem* 85:431–454.
19. Eriksson KK, Cervantes-Barragán L, Ludewig B, Thiel V (2008) Mouse hepatitis virus liver pathology is dependent on ADP-ribose-1″-phosphatase, a viral function conserved in the alpha-like supergroup. *J Virol* 82(24):12325–12334.
20. Fehr AR, et al. (2015) The nsp3 macrodomain promotes virulence in mice with coronavirus-induced encephalitis. *J Virol* 89(3):1523–1536.
21. Putics A, Filipowicz W, Hall J, Gorbalenya AE, Ziebuhr J (2005) ADP-ribose-1″-monophosphatase: A conserved coronavirus enzyme that is dispensable for viral replication in tissue culture. *J Virol* 79(20):12721–12731.
22. Kuri T, et al. (2011) The ADP-ribose-1″-monophosphatase domains of severe acute respiratory syndrome coronavirus and human coronavirus 229E mediate resistance to antiviral interferon responses. *J Gen Virol* 92(Pt 8):1899–1905.
23. Fehr AR, et al. (2016) The conserved coronavirus macrodomain promotes virulence and suppresses the innate immune response during severe acute respiratory syndrome coronavirus infection. *MBio* 7(6):e01721-16.
24. Daniels CM, Ong S-E, Leung AKL (2014) Phosphoproteomic approach to characterize protein mono- and poly(ADP-ribosyl)ation sites from cells. *J Proteome Res* 13(8): 3510–3522.
25. Rosenthal F, et al. (2013) Macrodomain-containing proteins are new mono-ADP-ribosylhydrolases. *Nat Struct Mol Biol* 20(4):502–507.
26. Jankevicius G, et al. (2013) A family of macrodomain proteins reverses cellular mono-ADP-ribosylation. *Nat Struct Mol Biol* 20(4):508–514.
27. Li C, et al. (2016) Viral macro domains reverse protein ADP-ribosylation. *J Virol* 90(19): 8478–8486.
28. Hottiger MO, Hassa PO, Lüscher B, Schüler H, Koch-Nolte F (2010) Toward a unified nomenclature for mammalian ADP-ribosyltransferases. *Trends Biochem Sci* 35(4): 208–219.
29. Gibson BA, Kraus WL (2012) New insights into the molecular and cellular functions of poly(ADP-ribose) and PARPs. *Nat Rev Mol Cell Biol* 13(7):411–424.
30. Vyas S, et al. (2014) Family-wide analysis of poly(ADP-ribose) polymerase activity. *Nat Commun* 5:4426.
31. Daniels CM, Ong S-E, Leung AKL (2015) The promise of proteomics for the study of ADP-ribosylation. *Mol Cell* 58(6):911–924.
32. Leidecker O, et al. (2016) Serine is a new target residue for endogenous ADP-ribosylation on histones. *Nat Chem Biol* 12(12):998–1000.
33. Rosenthal F, Hottiger MO (2014) Identification of ADP-ribosylated peptides and ADP-ribose acceptor sites. *Front Biosci (Landmark Ed)* 19:1041–1056.
34. Daniels CM, Thirawatananond P, Ong S-E, Gabelli SB, Leung AKL (2015) Nudix hydrolases degrade protein-conjugated ADP-ribose. *Sci Rep* 5:18271.
35. Palazzo L, et al. (2015) Processing of protein ADP-ribosylation by Nudix hydrolases. *Biochem J* 468(2):293–301.
36. Palazzo L, et al. (2016) ENPP1 processes protein ADP-ribosylation in vitro. *FEBS J* 283(18):3371–3388.
37. Malet H, et al. (2009) The crystal structures of Chikungunya and Venezuelan equine encephalitis virus nsP3 macro domains define a conserved adenosine binding pocket. *J Virol* 83(13):6534–6545.
38. Karras GI, et al. (2005) The macro domain is an ADP-ribose binding module. *EMBO J* 24(11):1911–1920.
39. Neuvonen M, Ahola T (2009) Differential activities of cellular and viral macro domain proteins in binding of ADP-ribose metabolites. *J Mol Biol* 385(1):212–225.
40. Egloff M-P, et al. (2006) Structural and functional basis for ADP-ribose and poly(ADP-ribose) binding by viral macro domains. *J Virol* 80(17):8493–8502.
41. Kistemaker HAV, et al. (2016) Synthesis and macrodomain binding of mono-ADP-ribosylated peptides. *Angew Chem Int Ed Engl* 55(36):10634–10638.
42. Zhang W, et al. (2015) Structural insights into the mechanism of Escherichia coli YmdB: A 2′-O-acetyl-ADP-ribose deacetylase. *J Struct Biol* 192(3):478–486.
43. Gorchakov R, et al. (2012) Attenuation of Chikungunya virus vaccine strain 181/clone 25 is determined by two amino acid substitutions in the E2 envelope glycoprotein. *J Virol* 86(11):6084–6096.
44. Otsuki K, Maeda J, Yamamoto H, Tsubokura M (1979) Studies on avian infectious bronchitis virus (IBV). III. Interferon induction by and sensitivity to interferon of IBV. *Arch Virol* 60(3-4):249–255.
45. Ashbrook AW, et al. (2014) Residue 82 of the Chikungunya virus E2 attachment protein modulates viral dissemination and arthritis in mice. *J Virol* 88(21): 12180–12192.
46. Atasheva S, Akhrymuk M, Frolova EI, Frolov I (2012) New PARP gene with an anti-alphavirus function. *J Virol* 86(15):8147–8160.
47. Atasheva S, Frolova EI, Frolov I (2013) Interferon-stimulated PARPs are potent inhibitors of cellular translation and virus replication. *J Virol*, 10.1128/JVI.03443-13.
48. Daugherty MD, Young JM, Kerns JA, Malik HS (2014) Rapid evolution of PARP genes suggests a broad role for ADP-ribosylation in host-virus conflicts. *PLoS Genet* 10(5): e1004403.
49. Cashman NR, et al. (1992) Neuroblastoma x spinal cord (NSC) hybrid cell lines resemble developing motor neurons. *Dev Dyn* 194(3):209–221.